Simplified Fine-Motion Planning in Generalized Contact Space [1]

Gordon Dakin Robin Popplestone

COINS Technical Report 92-41

May 26, 1992

Laboratory for Perceptual Robotics
Department of Computer and Information Science
University of Massachusetts
Amherst, MA 01003

Abstract

A methodology is presented for planning fine-motions for assembly operations in the presence of position, velocity, and model uncertainty. A nominal assembly motion plan, computed without regard to the effects of uncertainty, is provided a priori. *The* critical points *where collisions and jamming are likely to occur are first identified in the nominal trajectory. The configuration space of the assembly is then linearized about each critical point, producing local, hyperpolyhedral contact spaces that provide simplified motion planning domains in which to synthesize piecewise-linear trajectories. The hyperpolyhedral contact spaces are constructed with extra dimensions, one for each toleranced assembly part parameter. A heuristic search is performed in these generalized contact spaces to select a fine-motion trajectory that can be executed in the presence of position, velocity, and model uncertainty without deviating from a predictable sequence of contact states. A hybrid control strategy is then generated for traversing each contact state in the sequence.*

[1]Preparation of this paper was supported by grants CDA-8922572 and IRI-9023355 from the National Science Foundation.

1 Introduction

In the "two-phase" approach to fine-motion planning with uncertainty, a nominal trajectory is first computed in free space, without considering the effects of position, velocity, and model error, which are then accommodated in a second phase of planning. Accommodation of uncertainty in the second phase can involve the use of corrective compliance, in which forces on the moving part are made to relate to its position [26][31], velocity [14][24][30] or acceleration [2][15]. A carefully-chosen compliance behavior will map the contact forces that develop between the assembly parts to corrections in the moving part's trajectory. Another approach relies on the logical switching of control strategies, whereby deviations of the moving part from the nominal trajectory trigger error recovery strategies or patch-plans, which may be computed off-line [1][12] or on-line [8][32]. The prediction of assembly failure through simulation can also guide the iterative modification of the nominal trajectory or its initial conditions [3][20][28].

In the "single-phase" category of fine-motion planning techniques, contact space trajectories are synthesized "from scratch", without the benefit of a nominal trajectory provided *a priori*. Uncertainty considerations guide the selection of a fine-motion trajectory in the *generate and test* approaches [5][7][17], as well as the LMT methods [4][11][13][21]. In the former methods, candidate nominal motion plans are subjected to uncertainty analyses based on the forward-projection of pose uncertainty regions along the command trajectory, whereas the LMT methods employ backprojections or pre-images of uncertainty regions. Some contact space planning techniques do not deal with uncertainty directly [10][16][29], but attempt to restrict the assembly motion to the 1-dimensional facets of contact space, where executed motions are virtually free of uncertainty.

Other fine-motion planning research has focused on individual tasks, most notably the peg-in-hole task, for which applied force constraints have been derived [5][23][25][27][31] for preventing jamming (static friction) and wedging (sticking with part deformation) in the in the various contact states that might be encountered along an uncertain trajectory. In the approach of [5][6], the initial pose of the peg is perturbed to an off-center approach position, restricting the assembly motion to a predictable sequence of contact states, thereby simplifying the task of preventing jamming in each encountered contact state. The use of hybrid control to traverse contact states whose iden-

tities are known at the time of execution has also been explored [9][18][22], combining the precision of position control with the jamming-avoidance capabilities of force control.

This paper presents a "two-phase" approach to fine-motion planning with uncertainty. Building on a methodology previously developed [7], a nominal mating trajectory is first computed by a high-level assembly planner, such as *KA3* [19], without regard to the effects of uncertainty. The *critical points* are then identified in the nominal trajectory, signifying the "trouble spots" where jamming and collisions are likely to take place. The configuration space of the assembly is then linearized about each critical point, producing local contact spaces comprised of hyperplanar C-surfaces. The linearized contact spaces provide simplified domains in which to synthesize a piecewise-linear trajectory that will pass through a predictable sequence of contact states. Moreover, the local C-spaces may be constructed with extra dimensions for tolerances in the assembly part parameters. These *generalized C-spaces* are local, linearized versions of the one introduced by Donald [11]. Adopting a generate-and-test paradigm, candidate piecewise-linear trajectories are judged for reliability using an uncertainty analysis technique described in [7]. A heuristic search is performed in generalized contact space to select a trajectory that is optimal with respect to its reliability in the presence of uncertainty. Laugier [17] has also used a heuristic search of contact space to select fine-motion trajectories, but the representation of contact space, as well as the heuristics employed, bear little resemblance to those incorporated in the current approach. Finally, a hybrid control strategy is generated for each contact state traversed by the fine-motion trajectory.

2 An overview of the current approach

The nominal trajectory provided by the high-level planner translates a *moving part* relative to a *stationary part* from free space to a goal configuration. The nominal trajectory is derived geometrically from solid models whose dimensions do not allow for clearances at the insertion sites, so the moving part is not free to deviate from the nominal path. The moving part in figure 1, for instance, can neither rotate nor deviate laterally from its nominal trajectory, after the insertion has begun. With the introduction of clearances to the models, however, the moving part is free to move in a 6-dimensional

C-space, with 3 translational, and 3 rotational dimensions. The insertion clearances, which are specified by the designer of the assembly parts, are introduced just prior to the second phase of planning, which is the focus of this paper.

The present approach adopts the robotic assembly paradigm in which the moving part is first servoed visually to an initial pose in free space, and then translated along a specified sliding trajectory toward a goal relationship with the stationary part. Due to visual positioning error and control velocity error, the moving part's trajectory deviates laterally from the command trajectory, and the assembly may fail to reach the goal configuration if the command trajectory is not chosen with regard to the effects of uncertainty. Jamming or wedging can also develop in the course of the sliding motion if precautions are not taken to avoid static friction conditions in each contact state that might be encountered. In order to manage the uncertainty involved in the moving part's trajectory and simplify the problem of jamming avoidance, our fine-motion planner synthesizes a command trajectory that restricts the path of the assembly to a predetermined sequence of contact states. An uncertainty analysis is performed to determine if a candidate trajectory can be executed in the presence of uncertainty in the initial pose, velocity, and dimensions of the assembly parts without deviating from the chosen sequence of contact states.

The "trouble spots" where collisions can occur during the assembly operation are called the *critical points* (CPs) in the trajectory (see figure 1). These are just the configurations where the set of contacting surface features changes along the nominal trajectory, when clearance-free solid models are involved. Given a nominal trajectory and a pair of solid models with nonzero clearances, the goal of the second phase of fine-motion planning is to formulate a fine-motion plan to successfully maneuver the moving part through the 6-dimensional C-spaces associated with the CPs. Between the CPs, the trajectory can usually be confined to a 1-D crevice of contact space, minimizing uncertainty in the moving part's trajectory. Therefore, our fine-motion planning method focuses on the more troublesome CPs, and trajectory planning takes place within the local contact space surrounding each CP.

The local 6-dimensional C-space surrounding a CP is bounded by 5-dimensional C-surfaces, each of which corresponds to a *primitive contact* that can occur at the CP (see figure 2). For polyhedral objects, each primitive contact is a single-point contact involving either a convex vertex and a face,

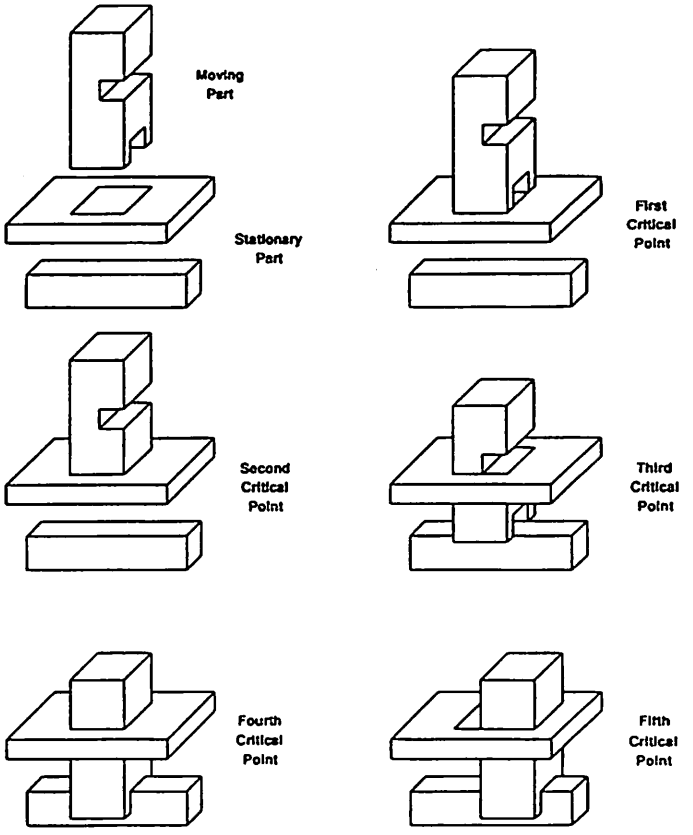

Figure 1: The critical points in a nominal trajectory.

or two convex edges. Pairs of primitive contacts that can occur simultaneously correspond to the 4-dimensional contact states, i.e., the 4-dimensional facets of contact space. In general, n primitive contacts restrict n of the moving part's 6 *dofs*, confining its pose to a $6-n$-dimensional contact state, i.e., a $6-n$-dimensional facet of contact space (see Koutsou [16]).

To support the search for an optimal sequence of contact states within each CP's local contact space, each contact space is constructed as an adjacency graph of contact states, implicitly representing all of the possible sequences of contact states in a fine-motion plan. Since it is unrealistic to attempt to establish or separate two or more primitive contacts at exactly the same time, a pair of contact states is only considered adjacent if their dimensionality differs by one. Consequently, any sequence of contact states selected from the graph will involve contact state transitions requiring the

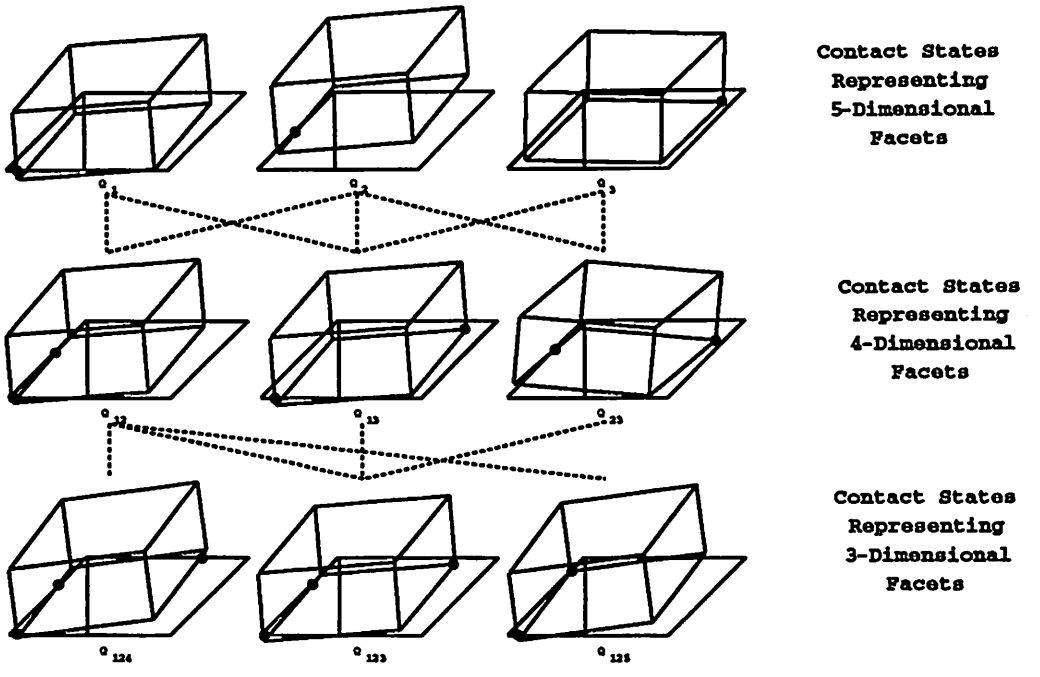

Figure 2: Adjacency graph of contact states at a critical point.

establishment or separation of exactly one primitive contact at a time.

Assuming the insertion clearances are small, as is usually the case in industrial assemblies, the local contact space around each CP is approximately hyperpolyhedral. As described in section 3, a hyperpolyhedral representation of each CP's C-space is derived by linearizing each C-space around its CP configuration. A candidate fine-motion plan for traversing the local contact space surrounding a CP consists of a specified sequence of contact states, together with a piecewise-linear trajectory through the specified states' hyperpolyhedral approximations. Each candidate trajectory is subject to an uncertainty analysis, to determine if its associated sequence of contact states can be successfully traversed in the presence of initial position, velocity, and model error. In order to perform uncertainty analysis incorporating model error, each hyperpolyhedral contact space is constructed in a higher-dimensional, *generalized C-space* with extra dimensions for variable model parameters (see Donald [11]).

By verifying through uncertainty analysis that only a preselected sequence of contact states will be traversed, the identity and geometry of each successive contact state will generally be known at the time of execution.

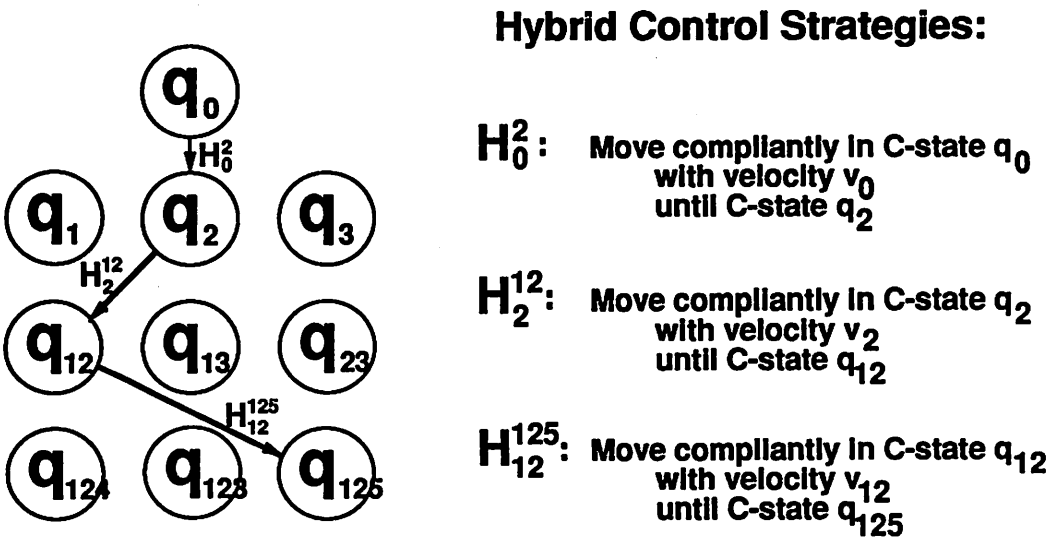

Figure 3: Hybrid control strategies for traversing contact states.

This enables us to utilize hybrid control for traversing the selected contact states, whereby the n surface tangents of an n-dimensional contact state are position-controlled, while the remaining $6-n$ are force-controlled. As shown in figure 3, a hybrid control strategy is specified for each contact state in the fine-motion plan in terms of the contact state to be traversed and the command velocity to execute in that state, plus a termination predicate, to signal the hybrid control strategy for the next contact state. The piecewise-linear trajectory determines each command velocity, and each subsequent contact state's force signature supplies the termination predicate.

A heuristic search is employed to select efficiently the best sequence of contact states and target points for traversing a CP's C-space. A cost function evaluates the relative merits of alternative piecewise-linear trajectories and their associated contact state sequences. The cost of a trajectory depends on (1) the number of contact state transitions involved, (2) the likelihood that the assembly will deviate from the selected path of contact states (as revealed through uncertainty analysis), and (3) the difficulty in distinguishing the force signatures of sequential contact states from each other, and from likely "error states" outside of the sequence.

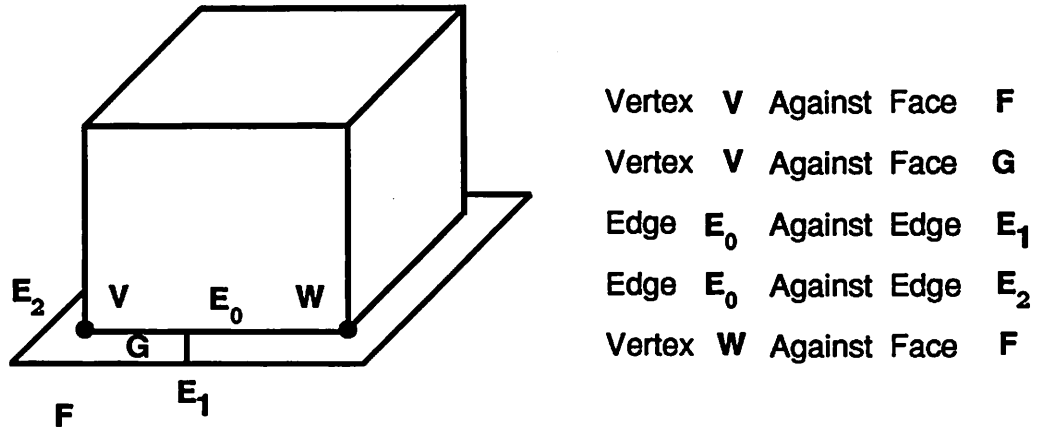

Figure 4: Some primitive contacts at a critical point.

3 Building the contact state adjacency graph

A contact state adjacency graph is constructed to represent the topology of the local C-space surrounding each CP. The construction of each CP's contact state graph begins with the enumeration of the *primitive contacts* that can occur around the CP (see figure 4). The primitive contacts that can occur in the presence of insertion clearances are just the primitive contacts that occur simultaneously prior to introducing clearances to the object models. To form a hyperpolyhedral approximation of each local contact space, the 5-D C-surfaces associated with the primitive contacts are approximated by 5-D hyperplanes. Assuming the insertion clearances are small, this is a fairly accurate approximation.

Moreover, in order to perform uncertainty analysis involving toleranced model parameters, the hyperpolyhedral contact spaces are formed in a generalized C-space with extra dimensions for model parameters. The geometry of a vertex-face contact with toleranced surface feature locations is shown in figure 5. The position of vertex V is modelled as a displacement $\mathbf{r}$ from the part's origin $\mathbf{p}$. The actual position of the vertex is represented by an uncertain displacement $\mathbf{dr}$. Stationary part face F is located an unknown distance dr_G along normal $\mathbf{n}$ from its model position. The 6-dimensional C-space surrounding the CP is augmented with 4 extra dimensions for the model

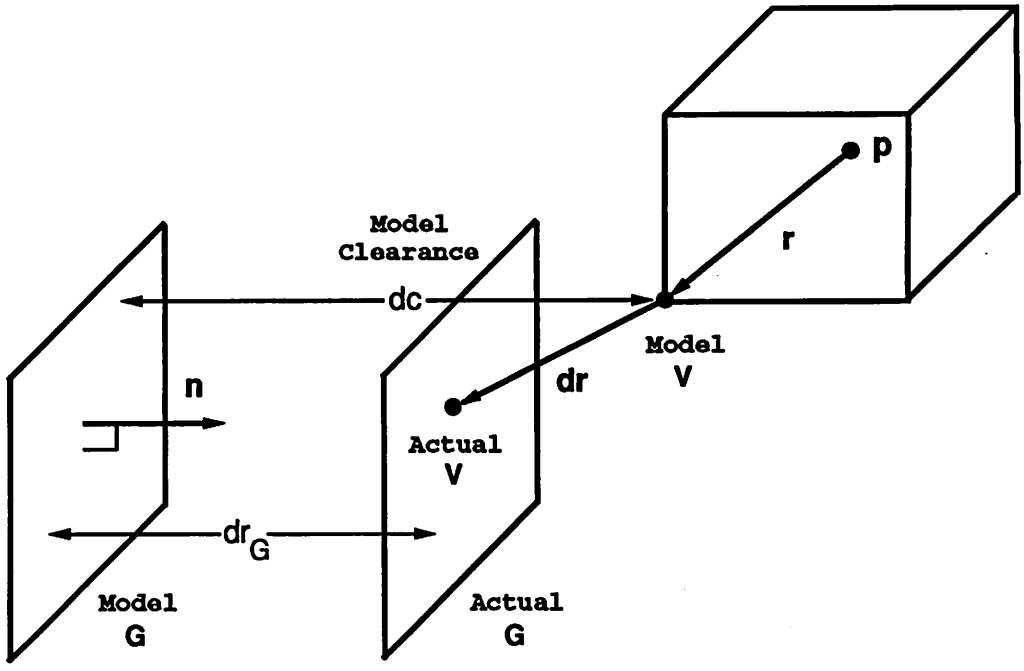

Figure 5: A vertex-face contact with model uncertainty.

parameters dr and dr_G, forming a generalized, 10-dimensional C-space. A 9-dimensional hyperplane for the vertex-face contact's generalized C-surface is expressed as a hyperplanar equation:

$$\begin{bmatrix} \mathbf{n} \\ \mathbf{r} \times \mathbf{n} \\ 1 \\ \mathbf{n} \end{bmatrix} \cdot \begin{bmatrix} \mathbf{dx} \\ \delta\mathbf{x} \\ dr_G \\ \mathbf{dr} \end{bmatrix} = -dc \tag{1}$$

where dx and δx denote the perturbed position and orientation of the moving part away from the CP, which serves as the origin of the local C-space.

In addition to a hyperplanar equality, a linearized C-surface description requires inequality constraints to represent the finite extent of the contacting surface features, as well as to prohibit overlapping configurations. The vertex-face contact shown in figure 6 has two inequalities denoting restricted

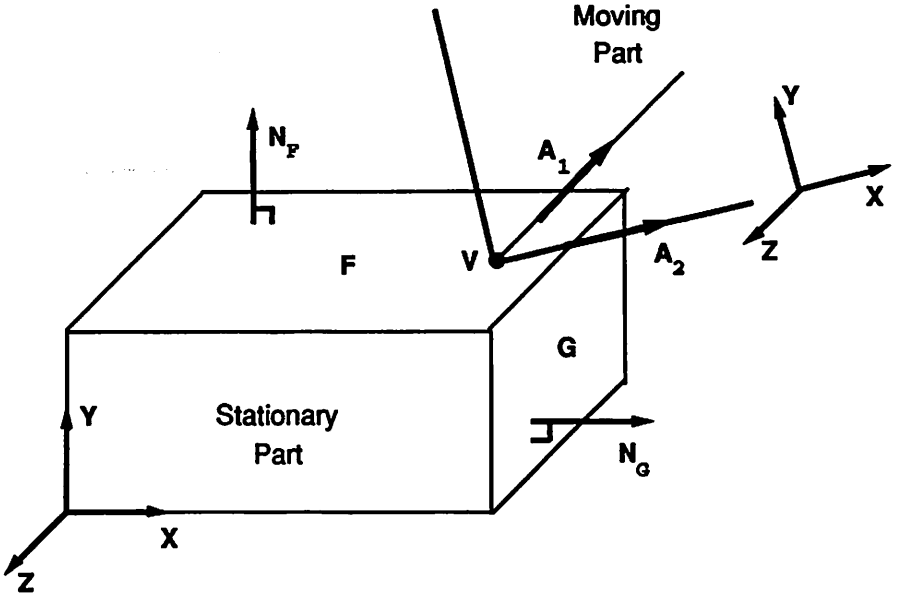

(a) Vertex V against face F
(b) Nonpositive rotation about axis $\mathbf{A}_1$
(c) Nonnegative rotation about axis $\mathbf{A}_2$
(d) Vertex V to the left of face G

$$
\begin{array}{lrcl}
(a) & 0.00\,dx + 0.65\,dy + 0.00\,dz + 0.36\,\delta x + 0.00\,\delta y - 0.65\,\delta z & = & 0.00 \\
(b) & 0.00\,dx + 0.00\,dy + 0.00\,dz + 0.00\,\delta x + 0.00\,\delta y - 1.00\,\delta z & \leq & 0.00 \\
(c) & 0.00\,dx + 0.00\,dy + 0.00\,dz - 1.00\,\delta x + 0.00\,\delta y + 0.00\,\delta z & \leq & 0.00 \\
(d) & 0.87\,dx + 0.00\,dy + 0.00\,dz + 0.00\,\delta x - 0.48\,\delta y + 0.00\,\delta z & \leq & -4.38
\end{array}
$$

Figure 6: Linear constraints for a vertex-face contact.

rotation about its adjacent edges (preventing overlap) and a single inequality restricting the vertex to lie on the finite planar surface of the face. The 4 combined linear constraints describe a convex polyhedral set in C-space. As it happens, no primitive contact's set of linear constraints contains more than 5 constraints, hence, each primitive contact's convex polyhedral set is devoid of vertices. This property of linearized C-surfaces is exploited in the uncertainty analysis technique described in section 4.

The convex polyhedral set associated with a primitive contact has a dual representation in the form of a weighted sum. Any point $\mathbf{P} \in \Re^6$ satisfying the single equality $\mathbf{N} \cdot \mathbf{P} = D$ and m inequalities $\mathbf{N}_i \cdot \mathbf{P} \leq D_i$ associated with

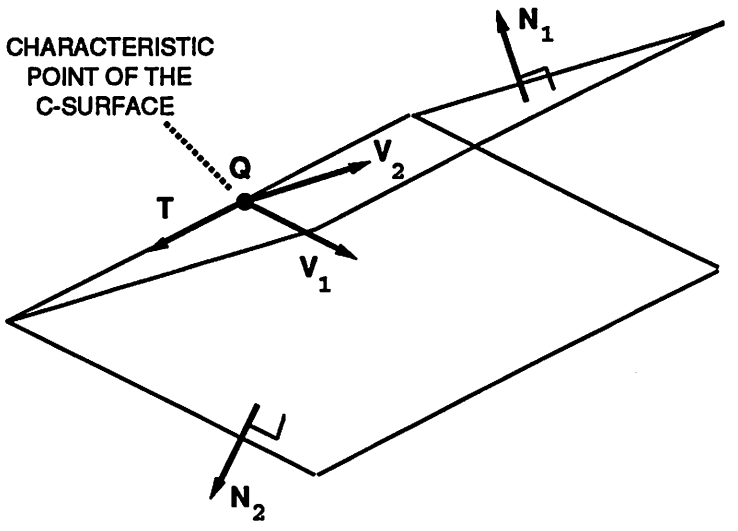

Figure 7: Convex cone characterization of a primitive contact.

a primitive contact can be expressed

$$\mathbf{P} = \mathbf{Q} + \Sigma_{i=1}^{m} \alpha_i \mathbf{V}_i + \Sigma_{j=1}^{6-m-1} \beta_j \mathbf{T}_j \ (\alpha_i \in \Re^+, \beta_j \in \Re) \qquad (2)$$

where the C-surface tangents $\mathbf{T}_1 \ldots \mathbf{T}_{6-m-1}$ span the vector space that is orthogonal to $span(\mathbf{N}, \mathbf{N}, \ldots, \mathbf{N}_m)$, and each surface tangent $\mathbf{V}_i$ is orthogonal to $\mathbf{N}, \mathbf{N}_1 \ldots \mathbf{N}_{i-1}, \mathbf{N}_{i+1} \ldots \mathbf{N}_m$ and $\mathbf{T}_1 \ldots \mathbf{T}_{6-m-1}$. The *characteristic point* $\mathbf{Q}$ of the C-surface satisfies the linear system $\mathbf{N} \cdot \mathbf{P} = D$, $\mathbf{N}_i \cdot \mathbf{P} = D_i$ $(i = 1 \ldots m)$, $\mathbf{T}_j \cdot \mathbf{P} = 0$ $(j = 1 \ldots 6 - m - 1)$. The tangent vectors are readily calculated via the Gram-Schmidt procedure. As figure 7 illustrates schematically in $\Re^3$, equation 2 describes a convex cone in $\Re^6$. By parameterizing equation 2 randomly, we may generate target points on the C-surface to serve as configurations defining candidate piecewise-linear trajectories.

A contact state adjacency graph is constructed by first placing a node in the graph for each primitive contact's 5-dimensional contact state, and then adding additional nodes for progressively lower-dimensional contact states. Target points are generated for each primitive contact state by parameterizing equation 2 randomly. As figure 8 shows schematically with 2-dimensional C-surfaces, exploratory tangent rays are cast along the 5-dimensional C-surfaces to find their adjacent, 4-dimensional contact states. This is accomplished by calculating every tangent ray's point of intersection with each remaining primitive contact's convex polyhedral set (if such an intersection exists), and then noting which intersecting primitive contact is encountered

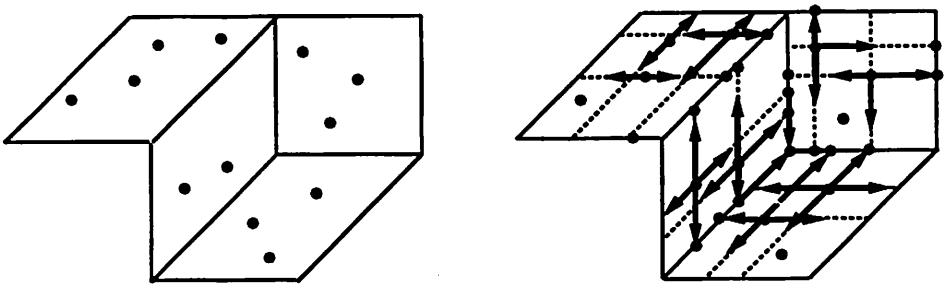

Figure 8: Generating target points in contact space.

first along each ray. Every adjacent C-state encountered in this manner is added to the adjacency graph, and the points of intersection between the tangent rays and adjacent primitive contacts are stored as target points in the new C-states. Exploratory tangent rays are, in turn, cast along the surfaces of the 4-dimensional C-states to discover their adjacent, 3-dimensional contact states, and so on. Each contact state is stored in the adjacency graph with a fixed number of target points, along with pointers to higher-dimensional "parents" and lower-dimensional "sons".

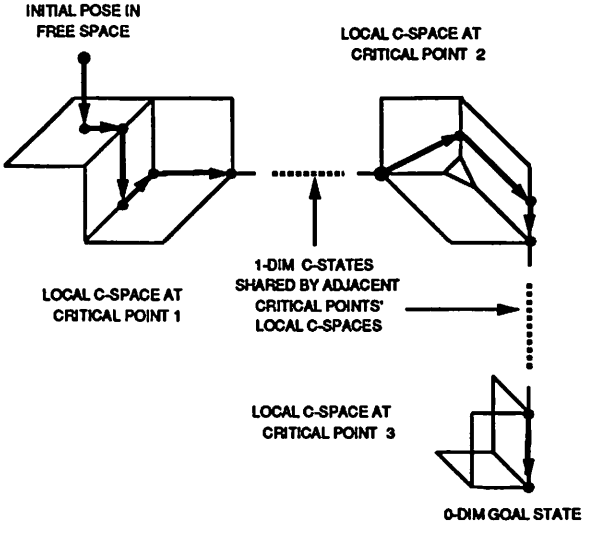

Figure 9: Piecewise-linear trajectories through local contact spaces.

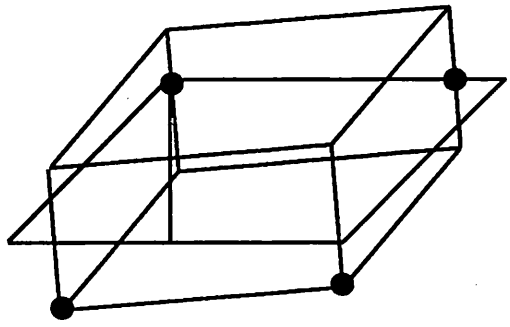

Figure 10: A 1-dimensional contact state between critical points.

4 Selecting a fine-motion plan

The contact state graph constructed for each CP's local contact space represents all the candidate sequences of contact states for traversing the contact space. A piecewise-linear trajectory is defined by first selecting a sequence of contact states and then choosing a target point for each chosen state (see figure 9). Fine-motion trajectories generated in this manner are evaluated with respect to their overall merit in a heuristic search of the contact state graph. A cost evaluation function incorporates the length of the contact state sequence, the likelihood that the assembly will deviate from the sequence, and the recognizability of each sequential contact state.

The local C-spaces surrounding adjacent CPs typically share a set of 1-dimensional contact states (see figure 10). The traversal of a concave 1-dimensional contact state is virtually free of uncertainty, since no *dofs* exist for lateral deviations arising from velocity error. As illustrated in figure 9, these 1-dimensional contact states serve as initial states and goal states when searching for alternative sequences of contact states in a local C-space. Exceptions to this rule are made in the case of the first CP, for which the initial state is always free space, and the last CP, where the goal state is always a 0-dimensional contact state associated with the final configuration supplied by the high-level planner. Once the initial states and goal states have been identified in a contact state adjacency graph, every contact state's minimum

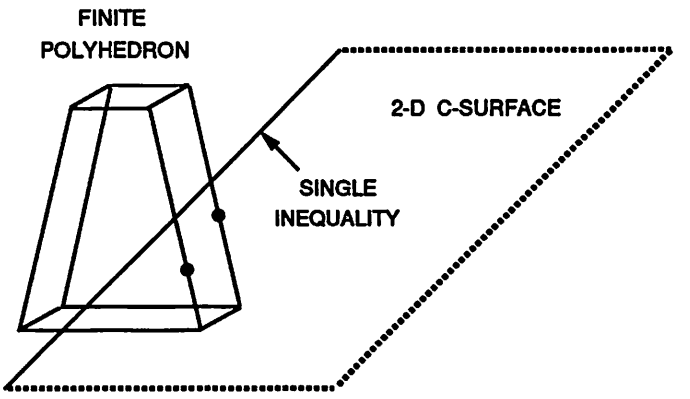

Figure 11: Intersecting a C-surface with a finite polyhedron.

distance to a goal state (i.e., the number of transitions required to reach a goal state) is calculated, to facilitate the search for a moderately short sequence of contact states through the local C-space.

Each candidate fine-motion trajectory is subject to an uncertainty analysis, to determine whether its execution can fail in the presence of initial position, velocity, and model uncertainty. The uncertainty analysis reveals possible deviations of the moving part from the prescribed sequence of contact states, as well as the margin of error involved in avoiding contact states outside the given sequence. The safety margin involved in avoiding unwanted contacts is used as a metric in the heuristic evaluation of a trajectory. The favoring of trajectories associated with a minimal likelihood of failure helps to counterbalance the effect of C-space linearization on the accuracy of the uncertainty analysis. Undesired contact state transitions associated with small safety margins are tabulated so that the undesired contact states' force signatures may be incorporated into error recovery stategies. The feasibility of distinguishing such undesired contact states' force signatures from the force signatures of the selected contact states is also included in the trajectory's heuristic evaluation.

As mentioned in section 3, the convex polyhedral set associated with each primitive contact has no vertices, since each polyhedral set is defined by a single inequality, and no more than 4 inequalities, in $\Re^6$. Our uncertainty analysis technique makes use of this fact to simplify the detection of linearized C-surface intersections with polyhedral uncertainty regions in 6-space and higher dimensions. Figure 11 illustrates an analogy in 3-dimensions, in which

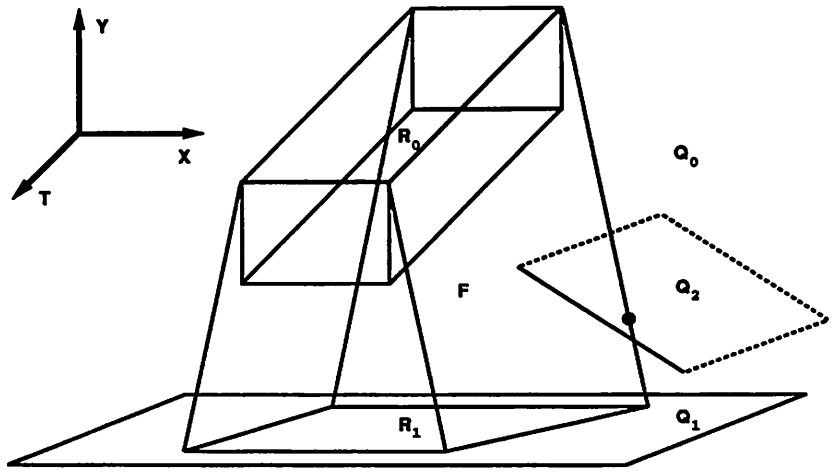

Figure 12: Uncertainty analysis in generalized contact space.

a half-planar C-surface intersects a polyhedron. Since the C-surface has no vertices, the C-surface cannot intersect the polyhedron without intersecting one of its linear edges. This observation generalizes to higher dimensions, simplifying the detection of an uncertainty region's intersection with any unwanted primitive contact's linearized C-surface. More costly methods of detecting intersections, such as linear programming feasibility tests, are thus avoided.

The piecewise-linear trajectory selected for traversing the first CP's local contact space starts at an initial pose in 6-dimensional free space. The moving part is visually servoed to the starting pose and then transported along the piecewise-linear command trajectory to the first selected contact state, then toward the second contact state, and so on. Figure 12 illustrates the uncertainty analysis procedure in lower dimensions. Uncertainty region $\mathbf{R_0}$, representing visual servo error, is formed in a 3-dimensional generalized C-space involving 2 pose dimensions X, Y and a single tolerance dimension T. $\mathbf{R_0}$ is projected along the first segment of the trajectory in free space $\mathbf{Q_0}$, toward the first selected contact state $\mathbf{Q_1}$. The forward-projection of $\mathbf{R_0}$ sweeps out a forward-projection volume $\mathbf{F}$ that expands laterally at a

rate which depends on the velocity uncertainty. To determine whether any contact state other than $\mathbf{Q_1}$ might be encountered along the first trajectory segment in the presence of uncertainty, intersections of $\mathbf{F}$ with any unwanted contact states are computed. As explained previously, a nonempty intersection between $\mathbf{F}$ and an unwanted contact state $\mathbf{Q_2}$ is detected efficiently by finding a linear edge of $\mathbf{F}$ that intersects $\mathbf{Q_2}$'s C-surface. If it is found that the first segment of the trajectory can be safely executed without encountering any unwanted contact states, $\mathbf{R_0}$'s projection $\mathbf{R_1}$ is recovered in contact state $\mathbf{Q_1}$, and the forward-projection process repeats recursively for the subsequent segments of the piecewise-linear trajectory.

Since uncertainty analysis is performed within a polyhedral approximation of contact space, and the precise ranges of position, velocity, and model uncertainty might be unavailable, unwanted contacts not predicted through uncertainty analysis may still occur. The forward-projections described above are therefore performed for several expanded ranges of uncertainty, to estimate the likelihood that unanticipated contact states will be encountered. The estimated likelihood that an unwanted contact will occur is inversely related to the degree of uncertainty required for a forward-projection volume to intersect the contact during uncertainty analysis.

Thus estimated, the likelihood that a fine-motion trajectory will fail in the presence of uncertainty provides one of the criteria for judging the "cost" of the trajectory, during the heuristic search for an optimal fine-motion plan. The difficulty in distiguishing the force signatures of unwanted contacts from those of planned contacts (for purposes of error recovery) provides another criterion for rating the relative merits of trajectories. Alternative piecewise-linear trajectories are thus evaluated, one linear segment at a time, in an A^* search which generates an optimal fine-motion plan.

5 Implementation and discussion

The fine-motion planner described above has been implemented in POP-11 and C running on a Sun-4 workstation. CSG descriptions of assemblies such as the one appearing in figure 1 are converted to surface boundary descriptions by the geometric solid modeller *ACIS*. The boundary descriptions of the assembly parts provide input to the high-level assembly planner *KA3* [19], as well as the fine-motion planner, which parametrizes C-surface equations

such as (1), using the geometric surface data. The high-level planner generates a nominal trajectory and a set of CPs for the fine-motion planner, and clearances and tolerances are selected for the surfaces of the assembly parts. [2] The fine-motion planner first constructs a contact state adjacency graph for each CP in the nominal trajectory, as described in section 3. The computation time for graph construction is roughly linear in the number of target points associated with each C-state. Since adjacent C-states are detected by comparing the proximities of different primitive contacts, as measured along surface tangent rays of existing C-states, the graph construction is also linear in the number of primitive contacts at the critical point. The construction of the C-state adjacency graphs for critical points of the assembly shown in figure 1 requires 5 to 10 minutes per graph on the Sun-4.

After the contact state graphs are constructed, the 1-dimensional contact states shared by neighboring CPs' graphs are identified and labelled as the initial states or goal states in the graphs. Each C-state's minimal distance to a goal state is then derived, requiring about one minute per graph. The heuristic search procedure constructs a search tree of partially-formed, piecewise-linear trajectories, with a branching factor of $O(ap)$, where a is the maximum number of C-state adjacencies involving a transition to a C-state of descreasing distance to a goal state, and p is the number of target points per C-state. In the worst case, the search for an optimal trajectory consisting of n linear segments requires $O((ap)^n)$ trajectory cost evaluations. In practice, the A^* search is rarely exhaustive, so the worst case complexity is seldom realized. For the critical points of the assembly shown in figure 1, the search for an optimal trajectory through a local C-space requires 2 to 6 minutes of run-time on the Sun-4, given $p = 12$ target points per C-state.

The computation time required to evaluate the cost of a piecewise-linear trajectory varies with the number of C-state adjacencies and the number of toleranced model dimensions. To determine whether any "error states" outside of the chosen sequence of C-states can be reached in the presence of uncertainty, the trajectory evaluation routine checks for intersections between the linear edges of a forward-projection volume and the convex polyhedral set of every primitive contact present in the possible error states but not in the

[2] In an industrial application, the clearances and tolerances would be selected by the designer of the assembly parts, based on function, performance, and machining cost constraints.

desired states. These intersections are perfomed are quite rapidly, owing to the convex polyhedral characterization of primitive contacts. The consequent computational simplicity of the uncertainty analysis procedure enables the fine-motion planner to perform thousands of trajectory evaluations in the course of a few minutes.

The number of facets in each pose uncertainty region is roughly exponential in the number of tolerances t (e.g., the initial pose uncertainty rectangle in free space has 2^{t+6} vertices), so the time required to calculate facet descriptors for a forward-projection volume **F** and a projected region **R** is also exponential in t. This method of uncertainty analysis is only practical when t is small (e.g.,$t \leq 10$).

Finally, the selected fine-motion trajectory maps directly to a sequence of hybrid control strategies and force signatures. Force signatures are also output for error states outside of the chosen sequence of C-states. As embodied in the heuristics for choosing a trajectory, the error state force signatures are easily distinguished from the trajectory C-states, facilitating on-line error recovery. A robotic implementation on a Zebra-0 robot is in progress.

6 Conclusion

A methodology for generating and testing fine-motion plans in generalized contact space was presented. The assumption of small insertion clearances enabled us to form simplified, hyperpolyhedral approximations of contact space around the critical points in a nominal assembly path. The rapid detection of intersections involving polyhedral uncertainty regions and linearized C-surfaces made it possible to generate and test a large number of alternative trajectories efficiently, to produce a fine-motion plan that can be executed in the presence of position, velocity, and model error.

7 References

1. Asada, H., Hirai, S. (1989), "Towards a symbolic-level force feedback: recognition of assembly process states", *Proceedings of the 5th International Symposium of Robotics Research, Tokyo, 1989.*

2. Asada, H., Kakumoto, Y. (1988), "The dynamic RCC hand for high-speed assembly", *Proceedings of the IEEE International Conference on Robotics and Automation*, pp.120-125.

3. Brooks, R.A. (1982), "Symbolic error analysis and robot planning", *Int. Journal of Robotics Research*, Vol. 1, No. 4 pp. 29-68.

4. Buckley, S,J. (1987), "Planning and teaching compliant motion strategies", PhD Thesis, M.I.T. Artificial Intelligence Laboratory, Cambridge, Mass. (also M.I.T. A.I. Lab T.R. 936).

5. Caine, M.E. (1985), "Chamferless assembly of rectangular parts in two and three dimensions", S.M. Thesis, Dept. of M.E., MIT.

6. Caine, M.E., Lozano-Pérez, T., Seering, W.P. (1989), "Assembly strategies for chamferless parts", *Proceedings of the IEEE International Conference on Robotics and Automation*, pp. 472-477.

7. Dakin, G., Popplestone, R.J. (1991), "Augmenting a Nominal Assembly Motion Plan with a Compliant Behavior", *Proceedings of the AAAI Conference*, Vol. 1, pp. 653-658.

8. Desai, R.S. (1987), "On Fine Motion in Mechanical Assembly in Presence of Uncertainty", Ph.D. Dissertation, Dept. of Mechanical Engineering., Univ. of Michigan.

9. De Schutter, J., Van Brussel, H. (1988), "Compliant robot motion I. A formalism for specifying compliant motion tasks", *International Journal of Robotics Research*, Vol. 7, No. 4, pp. 3 - 16.

10. Donald, B.R. (1984), "Motion planning with six degrees of freedom", Technical Report AI-TR-791, A.I. Laboratory, MIT.

11. Donald, B.R. (1986), "Robot motion planning with uncertainty in the geometric models of the robot and environment: a formal framework for error detection and recovery", *Proceedings of the IEEE Int. Conference on Robotics and Automation*, pp. 1588-1593.

12. Dufay, B., Latombe, J.C. (1984), "An approach to automatic robot programming based on inductive learning", *International Journal of Robotics Research*, Vol. 3, No. 4, pp. 3-20.

13. Erdmann, M. (1984), "On motion planning with uncertainty", Tech. Re-

port AI-TR-810, Artificial Intelligence Laboratory, MIT.
14. Hirai, S., Iwata, K. (1992), "A model-based generation of damping control law for part-mating", submitted to the IEEE International Conference on Intelligent Robots and Systems.
15. Kazerooni, H. (1988), "Direct-drive active compliant end effector (active RCC)", *International Journal of Robotics Research*, Vol. 4, No. 3, pp. 324-333.
16. Koutsou, A. (1986), "Parts mating by moving objects in contact", PhD Thesis, Dept. of A.I., Edinburgh University.
17. Laugier, C. (1989), "Planning fine motion stategies by reasoning in contact space", *Proceedings of the IEEE International Conference on Robotics and Automation*, pp.653-659.
18. Lee, C.S.G., Hou, E.S.H. (1988), "Automatic generation and synthesis of C-frames for mechanical parts in an insertion task", *Journal of Robotics and Automation*, Vol. 4, No. 3, pp. 287 -293.
19. Liu, Y. (1990), "Symmetry groups in robotic assembly planning", PhD Dissertation, COINS Dept., U.Mass., Amherst MA 01003.
20. Lozano-Pérez, T. (1976), "The design of a mechanical assembly system", Technical Report AI TR 397, AI. Lab, MIT.
21. Lozano-Pérez, T., Mason, M., Taylor, R.H. (1984), "Automatic synthesis of fine-motion strategies for robots", *International Journal of Robotics Research*, Vol. 3, No. 1, pp. 3-24.
22. Mason, M. (1981), "Compliance and force control for computer controlled manipulators", *IEEE Transactions on Systems, Man and Cybernetics*, Vol. SMC-11, No. 6, pp. 418-432.
23. Ohwovoriole, M.S. (1980), "An extension of screw theory and its applications to the automation of industrial assemblies", Stanford Artificial Intelligence Lab Memo AIM-338.
24. Peshkin, M.A. (1990), "Programmed compliance for error corrective assembly", *IEEE Transactions on Robotics and Automation*, Vol 6, No. 4, pp. 473-482.
25. Rajan, V.T., Burridge, R., Schwartz, J.T. (1987), "Dynamics of a rigid body in frictional contact with rigid walls", *Proceedings of the IEEE Int. Conference on Robotics and Automation*, pp. 671-677.
26. Salisbury, J.K. (1980), "Active stiffness control of a manipulator in Cartesian coordinates", *Proceedings of the 19th IEEE Conference on Decision and Control*, pp. 95-100.

27. Simunovic, S. (1975), "Force information in assembly processes", *Proc. of the 5th Int. Sym. on Industrial Robotics*, pp. 415-427.
28. Taylor, R.H. (1976), "A synthesis of manipulator control programs from task-level specifications", Stanford Univ., A.I. Lab., Memo AIM-282.
29. Valade, J. (1984), "Automatic generation of trajectories for assembly tasks", *Sixth European Conference on A.I.*, Pisa, Italy.
30. Whitney, D.E. (1985), "Historical perspective and state of the art in robot force control", *IEEE International Conference on Robotics and Automation*, pp. 262-268.
31. Whitney, D.E. (1982), "Quasi-static assembly of compliantly supported rigid parts", *Journal of Dynamic Systems, Measurement, and Control*, Vol. 104, pp. 64-77.
32. Xiao, J., Volz, R. (1988), "Design and motion constraints of part-mating planning in the presence of uncertainties", *Proceedings of the IEEE Int. Conference on Robotics and Automation*, pp.1260-1268.